Optimal Design of Transmission Characteristics for Hexagonal Coil Wireless Power Transfer System Based on Genetic Algorithm*

Ping'an Tan[1*], *Bin Song*[1], *Xu Shangguan*[1] *and Huadong Liu*[2]

(1. School of Automation and Electronic Information, Xiangtan University, Xiangtan 411105, China;
2. CRRC Zhuzhou Electric Locomotive Research Institute Co., Ltd., Zhuzhou 412001, China)

Abstract: Effective optimization methods are used to guide the optimal design of coil parameters, which is significant for improving the transmission performance of the wireless power transfer (WPT) system. Traditional methods mostly rely on the exhaustive attack method and finite element analysis (FEA) to achieve the coil parameter design, which have the disadvantages of complex modeling and time-consumption. To overcome these limitations, this study proposes an optimization strategy based on the genetic algorithm (GA), which considers the actual requirements of the efficiency and power of the WPT system. First, a direct integration method is proposed to simplify the analytical solution process of the mutual inductance between the hexagonal coils. Based on the mutual inductance model, the transmission characteristics of the hexagonal coil WPT system are deeply analyzed by the control variable method. Most importantly, with the proposed optimization objective function and its constraints, the GA is used to automatically achieve multi-parameter optimization of the hexagonal coil. Finally, a 500 W WPT system experimental platform is established, and the experimental results verify the feasibility of the proposed optimization method.

Keywords: Wireless power transfer (WPT), hexagonal coil, misalignment, optimal design, genetic algorithm (GA)

1 Introduction

Wireless power transfer (WPT) technology realizes the transmission of electrical energy from the power source to the load through magnetic fields, electric fields, electromagnetic waves, microwaves, and other media without wires, which significantly enhances the convenience of equipment movement, and has the advantages of safety, flexibility, intelligence, etc. Accordingly, coil misalignment caused by the randomness of the receiving side and the parameters of the coupling mechanism affect the performance of the WPT system, which poses numerous challenges in the maintenance of the efficient and stable operation of the WPT system [1-2]. Hence, it is necessary to establish an effective method to deeply analyze the influence of coil parameters on the transmission characteristics under actual working conditions and improve the overall performance of the WPT system through the optimal design of the parameters.

The existing coil design methods are mainly based on finite element analysis (FEA), the mutual inductance model, and the intelligent optimization algorithm to realize the optimization of the parameters. Among them, FEA requires simulation software such as ANSYS to simulate the coupling mechanism between coils under the action of multiple parameters through three-dimensional (3D) solid modeling, to determine the best working parameters of the coil. For example, the tolerance of rectangular coils [3] and DD coils [4] to misalignment was improved by the FEA of the influence mechanism of the coil parameters on their coupling coefficients. It is necessary for the FEA to re-model the coil structure when the coil parameters change, which increases the difficulty and time of modeling. To avoid the complicated modeling process, the mutual inductance model is used to optimize the parameters of the coaxial air-core solenoid [5] and the rectangular coil under misalignment conditions [6],

Manuscript received January 29, 2022; revised May 9, 2022; accepted August 4, 2022. Date of publication June 30, 2023; date of current version May 20, 2023.
* Corresponding Author, E-mail: tanpingan@126.com
* Supported by the Special Funding Support for the Innovative Construction in Hunan Province of China (2020GK2073).
Digital Object Identifier: 10.23919/CJEE.2023.000013

which improves the transmission efficiency of the WPT system. The above optimization process needs to scan all possible parameters through an enumeration method, and the optimization time is over-reliant on the dimension and accuracy of the parameters [7], which is not efficient enough. In recent years, intelligent optimization algorithms have been gradually applied to the optimal design of coil parameters. Compared with the traditional enumeration method, the parameter design of the circular coil using the Bayesian algorithm and the partial element equivalent circuit (BO-PEEC) approach [7] can improve the flexibility and efficiency of the design. By establishing a nonlinear programming model, the circular resonant coil of the dual-receiving WPT system is optimized based on the improved artificial bee colony algorithm, and the transmission efficiency reaches 94.29% under the rated power condition [8]. The research results show that the optimization algorithm can simultaneously achieve the multi-parameter optimization of coils with high speed and more accurate results. However, at this stage, the optimal design of coil parameters has been conducted mainly around typical circular, square and DD coils, and related research on the hexagonal coil is rarely involved. The hexagonal coil has the characteristics of seamless splicing and a flexible combination. Compared with the traditional circular and square array coils, the hexagonal array coil has better anti-misalignment characteristics, which improve the transmission efficiency and robustness of the WPT system [9]. Additionally, in the static and dynamic wireless charging system, the hexagonal coil demonstrates better cost-effectiveness than the circular or square coil [10]. When applied to the wireless charging of electric vehicles, the hexagonal coil can achieve a higher transmission efficiency with lighter weight than the circular coil under the same conditions [11]. Additionally, most of the existing coils are optimized to improve the system transmission efficiency without considering the actual power demand of the load. Therefore, it is necessary to further expand research on coil parameter optimization methods.

To improve the transmission characteristics of the hexagonal coil WPT system, a multi-parameter adaptive optimization strategy is proposed in this study. Compared with traditional optimization methods, the core contribution of the proposed method does not only consider the misalignment conditions, but also considers the actual requirements of the efficiency and power of the WPT system and uses the genetic algorithm (GA) to realize the automatic and rapid optimization of the coil parameters. Additionally, the calculation of the mutual inductance model is simplified based on the direct integration method, and the misalignment characteristics of the tangential and center boundaries of the hexagonal coil are deeply analyzed.

The rest of this paper is organized as follows. Section 2 presents the principle of the hexagonal coil WPT system. The mutual inductance modeling between hexagonal coils under misalignment is presented in Section 3. Section 4 analyzes the transmission characteristics of the hexagonal coils. Section 5 proposes the optimal design method. The experimental results are presented in Section 6.

2 Principle of the WPT system

2.1 Equivalent circuit

The WPT system based on the SS compensation network and two identical coil structures are discussed. The equivalent model is shown in Fig. 1. u_{in} is the AC input voltage; R_a is the internal resistance of the power source; L_s and L_p are the self-inductance of the transmitter (TX) and receiver (RX) coil, respectively; R_s and R_p are the internal resistances of the coils; C_s and C_p are the compensation capacitors on the primary and secondary sides, respectively; M is the mutual inductance between the coils, i_p and i_s are the transmitting and receiving side currents, respectively; R_L is the equivalent load; and u_{out} is the load voltage. In the case of resonance, the coil transmission efficiency η and output power P_o is defined as [12-14]

$$\eta = \frac{U_{out} I_s}{U_{in} I_p} = \frac{\omega^2 M^2 R_L}{(R_s + R_L)[\omega^2 M^2 + (R_s + R_L)(R_p + R_a)]} \quad (1)$$

$$P_o = R_L I_s^2 = \frac{U_{in}^2 \omega^2 M^2 R_L}{[(R_p + R_a)(R_s + R_L) + \omega^2 M^2]^2} \quad (2)$$

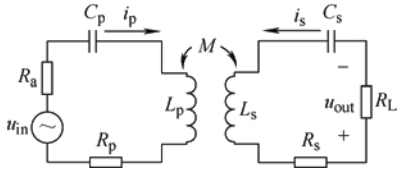

Fig. 1 Equivalent circuit model of the WPT system based on SS compensation

where U_{out} and U_{in} are the root mean square (RMS) values of the load and input voltage, respectively; I_p and I_s are the RMS values of the TX and RX coil currents, respectively; and ω is the angular frequency of the system. According to the analysis of Ref. [15], the equivalent internal resistance of the coil (R_p, R_s) at frequency f mainly includes the ohmic loss resistance R_o and the radiation loss resistance R_r, as shown in Eq. (3) and Eq. (4). In the case of a high frequency, $R_o >> R_r$, the Ohmic loss contains a high-frequency AC loss caused by the skin and proximity effects [16-17]; therefore, only the ohmic loss resistance is considered in the analysis of this study.

$$R_o = \frac{l}{\pi W_a}\sqrt{\frac{\pi f \mu_0}{\sigma}} \quad (3)$$

$$R_r = \sqrt{\frac{\mu_0}{\varepsilon_0}}\left[\frac{\pi}{12}n^2\left(\frac{\omega r_c}{c}\right)^4 + \frac{2}{3\pi^3}\left(\frac{\omega h_c}{c}\right)^2\right] \quad (4)$$

where l represents the wire length of the coil, W_a is wire diameter, μ_0 is the vacuum permeability, σ is the electrical conductivity, ε_0 is the relative permittivity, n is the number of turns of the coil, r_c is the radius of the coil, c is the speed of light, and h_c is the coil width.

2.2 Misalignment condition of the hexagonal coil

Considering the existing equivalent spiral coil transformation method [18], the hexagonal planar spiral coil is equivalently transformed as shown in Fig. 2. The t-th coil from the outside to the inside can be described as

$$c_t = c_1 - \frac{2\sqrt{3}}{3}\cdot(t-1)\cdot d_x \quad t = 1, 2, \cdots, N \quad (5)$$

where c_1 is the outermost side length, turn spacing $d_x = W_a + S_a$, S_a is the gap between two adjacent turns, W_a is the wire diameter, and N is the number of turns of the coil. The spatial distribution with the coil misalignment is shown in Fig. 2c, where i=1, 2, ⋯, N_p, j=1, 2, ⋯, N_s; N_p and N_s are the turns of the TX and RX coils, respectively; d is the transmission distance; and δ and ρ are the misalignment distances along the x-axis and y-axis, respectively.

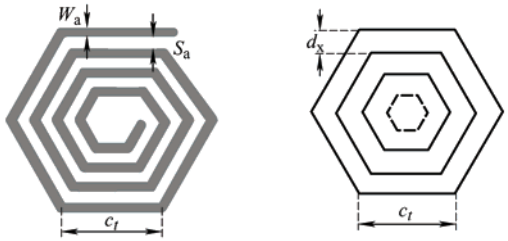

(a) Hexagonal planar spiral coil (b) Equivalent regular hexagonal coil

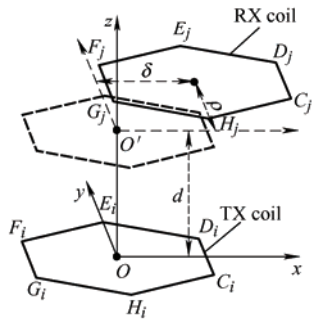

(c) Spatil distribution when the coil is misaligned

Fig. 2 Equivalent diagram of coils

According to Ref. [19], the central and tangential boundary directions of the hexagonal coils correspond to the x-axis and y-axis directions in Fig. 3a, respectively. The coordinate axis divides the hexagonal coil into four symmetrical regions, which are regions I, II, III, and IV respectively. The boundaries of the three symmetrical regions (I_1, I_2, and I_3) of region I are all composed of a tangential boundary and a central boundary. Based on this, the study mainly analyzes the misalignment conditions of the hexagonal coil along with the two boundary directions.

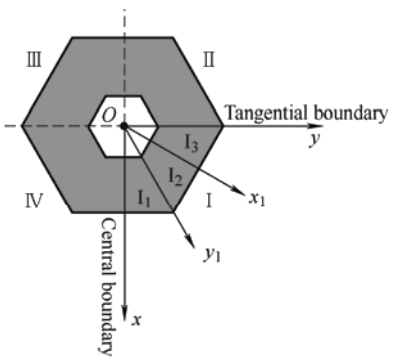

(a) Symmetrical region division of hexagonal coil

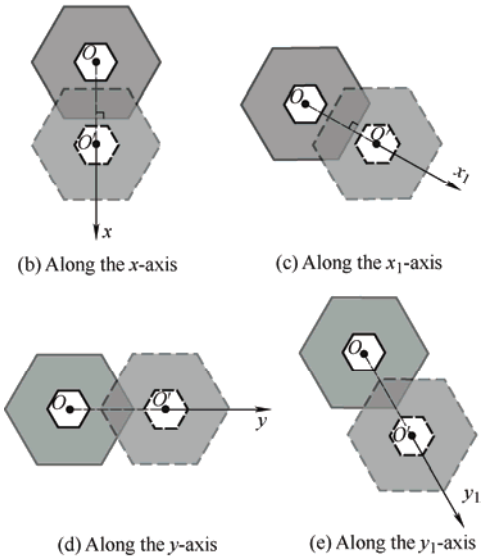

Fig. 3 Different horizontal misalignment conditions of hexagonal coils

3 Mutual inductance modeling of hexagonal coils under misalignment condition

3.1 Magnetic flux density

As shown in Fig. 2, when the two coils are parallel, the component of the magnetic flux density along the z-axis generated by the coils is considered. According to the Biot-Savart law, the magnetic flux density generated by the finite current-carrying wire C_iD_i at any point $W(x, y, z)$ in space can be derived as [20]

$$B_{C_iD_i}=\frac{u_0 I}{4\pi}\int_{C_iD_i}\frac{\sin\varphi \mathrm{d}\varphi}{r_0}=\frac{u_0 I}{4\pi r_0}\left(\cos\varphi_1+\cos\varphi_2\right) \tag{6}$$

where r_0 is the distance from point W to the current-carrying wire, $\varphi_1(\varphi_2)$ is the included angle between line segment C_iW(D_iW) and C_iD_i, and I is the current of the current-carrying wire. The relevant parameters are presented in Fig. 4. The component of the magnetic flux density $B_{C_iD_i}$ along the z-axis is represented as $B_{z\text{-}C_iD_i}=B_{C_iD_i}\cos\gamma$.

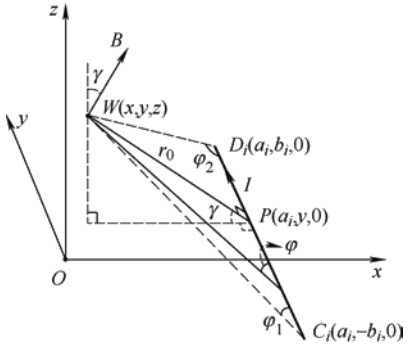

Fig. 4 Magnetic flux density of wire at any point in space

According to the coordinate axis rotation method in Ref. [21], the component of the magnetic flux density along the z-axis generated by each side of the i-th TX coil can be derived equivalently from Eq. (6), which can be expressed as

$$B_{zi\text{-}k}=\frac{u_0\beta_{i,k}I}{4\pi(\beta_{i,k}{}^2+z^2)}\left[\frac{b_i+y_k}{\sqrt{\beta_{i,k}{}^2+(b_i+y_k)^2+z^2}}+\frac{b_i-y_k}{\sqrt{\beta_{i,k}{}^2+(b_i-y_k)^2+z^2}}\right] \tag{7}$$

where $B_{zi\text{-}k}$ (k=1, 2, ⋯, 6) respectively represents the magnetic flux density generated by C_iD_i, D_iE_i, E_iF_i, F_iG_i, G_iH_i and H_iC_i in Fig. 2c, $\beta_{i,k}=a_i-x_k$, x_k and y_k are the coordinates of point W under the rotation coordinate axis [21]. The total magnetic flux density of the i-th TX coil at point W along the z-axis is defined as

$$B_{zi}=B_{z\text{-}C_iD_i}+B_{z\text{-}D_iE_i}+B_{z\text{-}E_iF_i}+B_{z\text{-}F_iG_i}+B_{z\text{-}G_iH_i}+B_{z\text{-}H_iC_i} \tag{8}$$

3.2 Mutual inductance

The magnetic flux density generated by the TX coil is not uniform within the area of the RX coil. The magnetic flux formula is rewritten as

$$\Phi=\int B\mathrm{d}S \tag{9}$$

To facilitate the calculation of the mutual inductance, each turn of the RX coil is divided into four integral areas, as shown in Fig. 5, and the linear equation corresponding to the four sides of D_jE_j, E_jF_j, G_jH_j, and H_jC_j is given. The equivalent division method of the integral region in Ref. [21] is slightly redundant, and the trapezoid area can be directly integrated according to the nature of the integration. The magnetic fluxes formed in the regions S_1 to S_4 are expressed as

$$\begin{cases}\Phi_{ij-1}=\int_{\delta}^{\frac{\sqrt{3}}{2}c_j+\delta}\int_{\rho}^{-\frac{\sqrt{3}}{3}(x-\delta)+c_j+\rho}B_{zi}\mathrm{d}y\mathrm{d}x\\ \Phi_{ij-2}=\int_{-\frac{\sqrt{3}}{2}c_j+\delta}^{\delta}\int_{\rho}^{\frac{\sqrt{3}}{3}(x-\delta)+c_j+\rho}B_{zi}\mathrm{d}y\mathrm{d}x\\ \Phi_{ij-3}=\int_{-\frac{\sqrt{3}}{2}c_j+\delta}^{\delta}\int_{-\frac{\sqrt{3}}{3}(x-\delta)-c_j+\rho}^{\rho}B_{zi}\mathrm{d}y\mathrm{d}x\\ \Phi_{ij-4}=\int_{\delta}^{\frac{\sqrt{3}}{2}c_j+\delta}\int_{\frac{\sqrt{3}}{3}(x-\delta)-c_j+\rho}^{\rho}B_{zi}\mathrm{d}y\mathrm{d}x\end{cases} \tag{10}$$

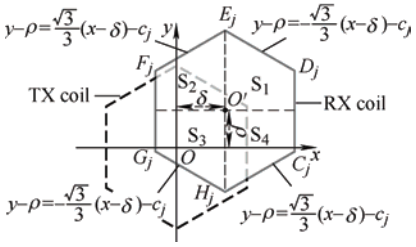

Fig. 5 Diagram of integration area under misalignment condition

The mutual inductance between the hexagonal planar spiral coils can be expressed as

$$M=\frac{\Phi}{I}=\frac{\sum_{i=1}^{N_P}\sum_{j=1}^{N_S}\left(\sum_{n=1}^{4}\Phi_{ij-n}\right)}{I} \tag{11}$$

The expression of the mutual inductance when the coil is misaligned along the tangential boundary or the central boundary can be simplified as

$$M_{|\delta=0}=\frac{2\sum_{i=1}^{N_P}\sum_{j=1}^{N_S}\left(\Phi_{ij-1}+\Phi_{ij-4}\right)}{I} \tag{12}$$

$$M_{|\rho=0}=\frac{2\sum_{i=1}^{N_P}\sum_{j=1}^{N_S}\left(\Phi_{ij-1}+\Phi_{ij-2}\right)}{I} \tag{13}$$

4 Transmission characteristics analysis for hexagonal coil WPT system

It is convenient to analyze the transmission characteristics of the WPT system coupling mechanism based on the mutual inductance model, which provides a theoretical basis for the optimal design of coupler parameters. In practical applications, the relevant parameters of the coupler such as the outside diameter, thickness, and shape of the coils are limited, and the load, output power level, and transmission efficiency of the WPT system are also required according to different requirements. This section analyzes the transmission characteristics of the hexagonal coil using the control variable method. The working environment of the WPT system specified in this paper is summarized in Tab. 1.

Tab. 1 Working environment of the WPT system

Parameter	Value
Switching frequency f/kHz	85
Output power P_o/W	500-550
Input voltage U_{in}/V	120(±10%)
Load R_L/Ω	30
Side length c_1/cm	18
Transmission distance d/cm	10

Combining the actual working environment, the wire type and wire diameter of the coil are first determined. The Litz wire is made up of several independent insulated conductors twisted together, which can reduce the skin effect and have a good high-frequency characteristic. Therefore, the Litz wire is selected as the material for winding the coil in this study. When high-frequency AC passes through a conductor, the current density decreases gradually from the surface to the center of the conductor owing to the skin effect of the current, and its depth of penetration is defined as [22]

$$\Delta=\sqrt{\frac{1}{\pi f\mu\sigma}} \tag{14}$$

where μ is the permeability of the wire. When the working frequency of the system is 85 kHz, it can be deduced from Eq. (14) that its depth of penetration is 0.22 mm. To weaken the skin effect of the current, the Litz wire was selected based on the principle that the single strand diameter was less than 2 times the depth of penetration; here, a single strand diameter of 0.1 mm is selected. Based on the study, the coil transmission efficiency should not be less than 95% under alignment. Considering the rated output power of 500 W, the rated current of the secondary side is 4.08 A based on Eq. (2). If the transmission efficiency is not less than 95%, according to Eq. (1), the maximum input power is 526.3 W, which means that the maximum primary current is 4.38 A when the input voltage is 120 V. Additionally, considering the margin of 1.5-2 times, this study finally chooses the Litz wire with a specification of 0.1 mm×220 turns, and its rated current is 8.65 A.

4.1 Analysis of misalignment characteristics

It is necessary to analyze the influence of the coil parameters on the misalignment characteristics before the optimal design. It is known that the mutual inductance M is a function of the coil parameters, which can be expressed as follows

$$M=f(N,c_1,d_x,W_a) \tag{15}$$

The side length and wire diameter of the coil have been determined; therefore, it is necessary to analyze the influence of N and d_x on the misalignment characteristics. Fig. 6 is the variation of the mutual

inductance between the coils with the misalignment distance at different N and d_x, including the misalignment along the tangential and central boundaries. The maximum misalignment distance is specified as 12 cm after considering the current withstand rating of the Litz wire. The calculated value of the mutual inductance model is compared with the finite element simulation value, and the result shows that the error is extremely small, which verifies the correctness of the mutual inductance model. It can be deduced that the mutual inductance is negatively correlated with the change of the misalignment distance, and the misalignment characteristics are determined by the coil parameters. The changes in the mutual inductance under the misalignment along two boundary directions are almost consistent by comparing Figs. 6a and 6b. Therefore, the next analysis and design process of coils mainly considers the misalignment along the tangential boundary as an example. Moreover, only the misalignment in the positive direction is considered based on the symmetry of the hexagonal coil.

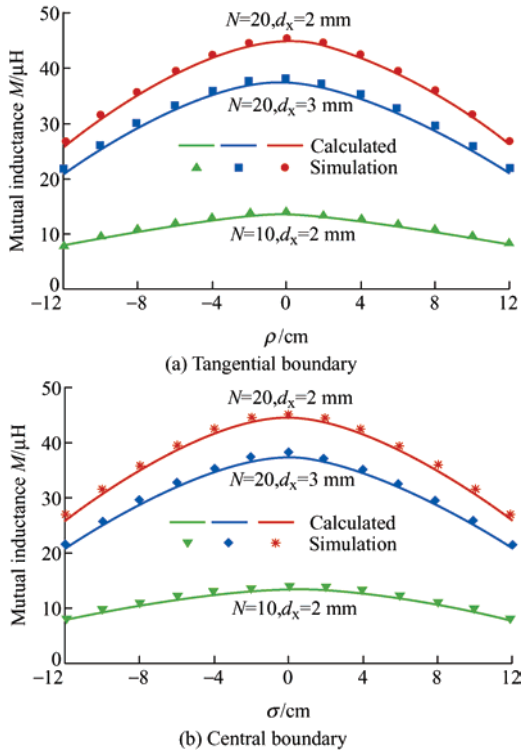

Fig. 6 Calculated value of mutual inductance of different coils under misalignment

It can be deduced from the efficiency Eq. (1) that the mutual inductance and efficiency have a non-linear relationship, as shown in Fig. 7a. As the mutual inductance increases, the transmission efficiency increases sharply at the beginning. However, when the mutual inductance value increases to a certain extent, the growth rate of the efficiency begins to level off with the increase of the mutual inductance. Therefore, the variation trend of the two with the misalignment distance is inconsistent, which can be obtained by comparing Fig. 6a and Fig. 7b. Further analysis of Eqs. (1), (2), (3) and (15) reveals that the coil parameters ultimately affect the transmission efficiency and output power, both of which should be considered in the optimal design of the coils so that better transmission characteristics are reflected.

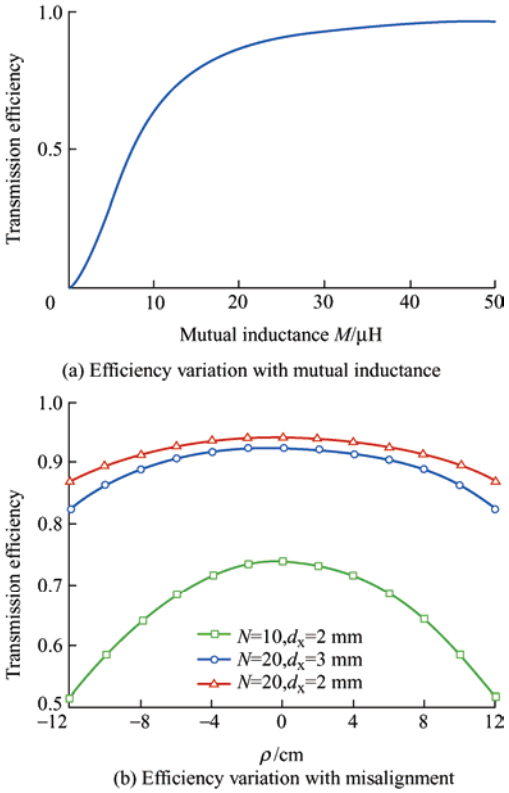

Fig. 7 Calculated value of transmission efficiency variation with mutual inductance and misalignment

4.2 Analysis of transmission efficiency and output power

Tab. 1 illustrates that the system output power ranges from 500 W to 550 W, and this section shows that the expected transmission efficiency of this study is above 95%. Therefore, the functional relationship between the coil parameters (N, d_x) and the efficiency and power can be obtained by combining the mutual

inductance model, coil internal resistance Eq. (3), transmission efficiency Eq. (1) and output power Eq. (2), such that the efficiency and power can be calculated. Data that meet the requirements can be calculated based on the limits of the efficiency and power, as shown in Fig. 8. The figure contains all the coil parameters that meet the work requirements. It can be observed from Fig. 8 that the efficiency trend is easier to observe; a larger number of coil turns N and a smaller turn spacing d_x cause a higher transmission efficiency, but the growth rate of the efficiency gradually tends to level off. However, the trend of the output power is difficult to determine, which requires further analysis of the original data. Moreover, to further obtain the coil parameters with the best transmission characteristics after determining all the parameters that meet the working requirements, it is necessary to plot the curve of the change of the transmission efficiency of all the coils with the misalignment distance by calculation before making further inferences, which is too complicated to implement. Hence, an optimal design process is proposed in the next section to obtain the coil parameters with the best transmission characteristics efficiently and accurately.

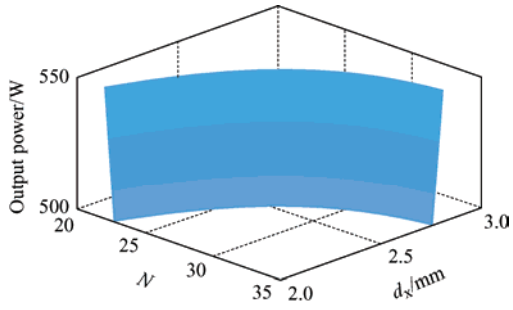

(a) Output power

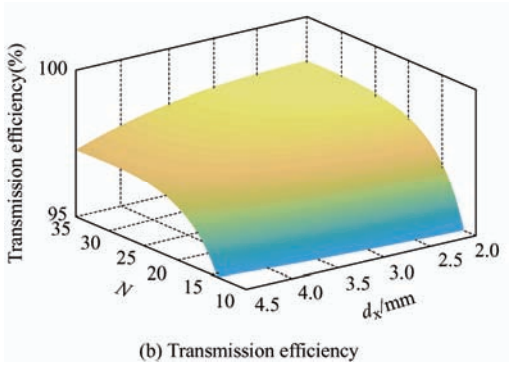

(b) Transmission efficiency

Fig. 8 Calculated values of transmission efficiency and output variation with coil parameters

5 Proposed optimal design method of hexagonal coil

This section proposes an efficient and accurate optimal design method of the coil parameters. The power transmission loss of the coils under misalignment is converted into a mathematical model, which is embodied in the form of an objective function. Taking the working conditions as the constraints, the GA is used to find the best solution of the objective function within the constraints, which consists of the coil parameters with the best transmission characteristics under misalignment. The optimization tool used is Matlab software.

5.1 Objective function

The key to the design is to ensure the optimal coupling state at every possible misalignment position and transform it into a mathematical model to facilitate the search for the optimal solution. The optimal transmission efficiency is undoubtedly the ultimate goal of the design and the best choice of the objective function. From this, the problem can be transformed into determining the optimal efficiency curve that varies with the misalignment distance, and the factors affecting this curve are the parameters N and d_x of the coil to be optimized. The efficiency curve function under the misalignment condition is set as $\eta(N, d_x, \rho)$, as shown in Fig. 9. The efficiency does not fluctuate up and down within a certain misalignment range but decreases gradually with the increase of the misalignment distance in a certain trend, and there is a fixed upper limit of the efficiency under any conditions, which is 1. Therefore, there are two options for obtaining the optimal efficiency curve by analyzing Fig. 9.

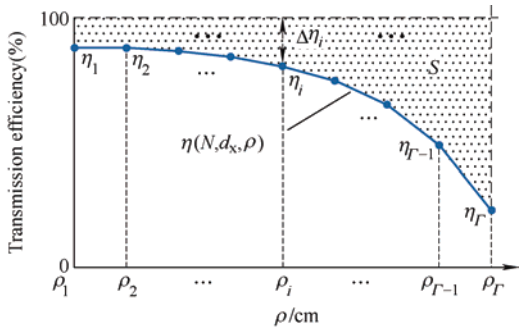

Fig. 9 Efficiency curve determined by the parameters N and d_x under misalignment conditions

Option 1: Minimize area S.

$$S=\int_{\rho_1}^{\rho_\Gamma}\left[1-\eta(N,d_{\mathrm{x}},\rho)\right]\mathrm{d}\rho \tag{16}$$

where ρ_i (i=1, 2, ⋯, Γ) represents the misalignment test point, and Γ is the number of the misalignment test point.

Option 2: Minimize the $\Delta\eta_i$.

$$\Delta\eta_i=1-\eta_i \tag{17}$$

where $\Delta\eta_i$ is the proportion of the coil transmission loss power to the total input power.

The calculation of area S needs to use the integral method, and the mutual inductance model in the efficiency formula includes an integral operation, which increases the difficulty of calculation. Therefore, option 2 is easier to implement.

Because of the randomness of the misalignment position, the concept of the RMS value is introduced to deal with option 2 to better reflect the transmission characteristics of the coil under misalignment. The final objective function is shown in Eq. (18), whose solution of the minimum value is the coil parameters with the optimal transmission characteristics.

$$fitness=\sqrt{\frac{\sum_{i=1}^{\Gamma}(\Delta\eta_i)^2}{\Gamma}} \tag{18}$$

5.2 Constraint condition

The constraint condition can be obtained directly according to Tab. 1 and the relationship between the coil parameters, as shown in Eq. (19), where g_2 aims to make the optimization result of d_{x} accurate to one digit after mm (as the unit in Matlab is unified as the meter but the value of d_{x} is on the millimeter level). $P_{\mathrm{o}}|_{\delta=0;\rho=0}$ and $\eta|_{\rho=0;\delta=0}$ represent the output power and transmission efficiency when the coils are aligned, respectively.

$$\text{s.t.}\begin{cases} g_1=N\in\boldsymbol{N}_+ \\ g_2=10\,000d_{\mathrm{x}}\in\boldsymbol{N}_+ \\ g_3=N\cdot W_{\mathrm{a}}-\dfrac{\sqrt{3}}{2}\cdot c_1\leqslant 0 \\ g_4=(N-1)\cdot d_{\mathrm{x}}+W_{\mathrm{a}}-\dfrac{\sqrt{3}}{2}\cdot c_1\leqslant 0 \\ g_5=0.95-\eta|_{\delta=0;\rho=0}\leqslant 0 \\ g_6=500-P_{\mathrm{o}}|_{\delta=0;\rho=0}\leqslant 0 \\ g_7=P_{\mathrm{o}}|_{\delta=0;\rho=0}-550\leqslant 0 \end{cases} \tag{19}$$

5.3 Coil optimization with GA

The optimization algorithm can be used to optimize the minimum value of the *fitness* because of the complexity of the function. The GA is used to determine the minimum value of the objective function as the overall search strategy and the optimization search method of the GA does not depend on the gradient information or other auxiliary knowledge, but only needs the objective function and the corresponding fitness function that affect the search direction. The optimization process is shown in Fig. 10. The GA toolbox of Matlab software is selected as the optimization tool. The optimal solutions obtained are N=23 and d_{x}=2.2 mm.

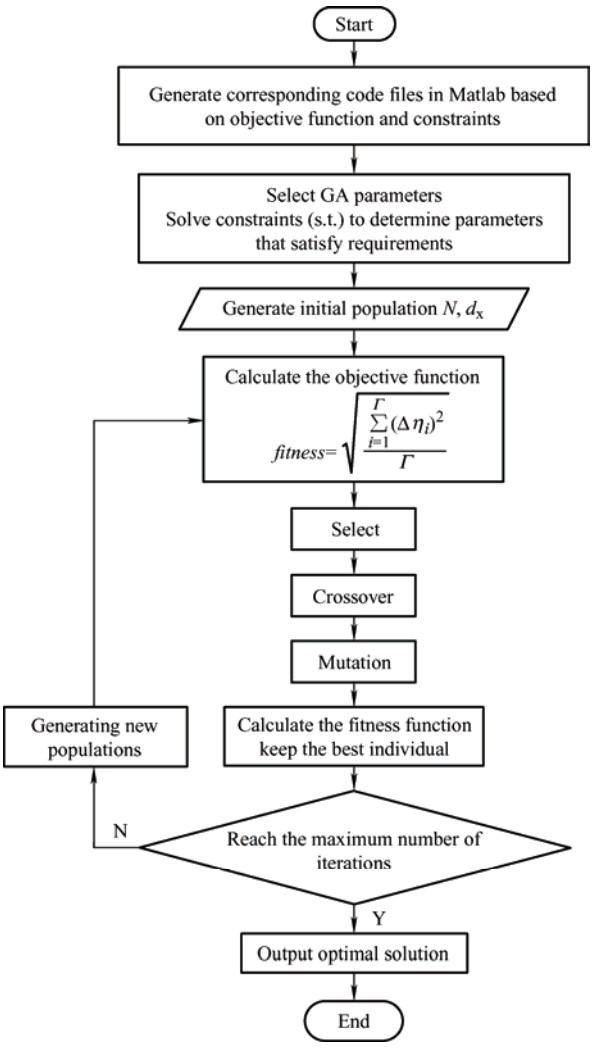

Fig. 10 Optimization flowchart of GA

The specific process of Fig. 10 is as follows.

Step 1: Convert the mutual inductance model and efficiency formula into Matlab code and establish the objective function file (Fitness.m) and constraint file

(Constraint.m).

Step 2: Set the running parameters of the GA as follows: population size 50, number of variables 2, maximum number of generations 200, generation gap value 0.95.

Step 3: The GA toolbox selects Fitness.m to calculate the fitness function.

Step 4: Selection, crossover, and mutation are three kinds of genetic operators of the basic GA. Among them, the proportional selection operator causes the chromosomes with high fitness to be the most likely to be selected. Consequently, excellent individuals can be selected from the old population, and crossover operations can be performed to obtain new population individuals. The selection function is a random uniform distribution function, the crossover probability is 0.8, and the variation function is a Gaussian function. The fitness value of each individual in the population is calculated and the best individual is saved.

Step 5: Determine whether the maximum number of iterations is reached, if so, output the optimal solution; otherwise, generate a new population and return to Step 4 to continue the calculation.

Based on the mutual inductance model and the efficiency Eq. (1), the variation of the transmission efficiency with the misalignment distance of all the coils that meet the working requirements can be calculated (exhaustive attack method). All the coil parameters included in Fig. 8 meet the working requirements. The data in Fig. 8 can be extracted using a drawing tool (Matlab) to obtain the specific coil parameters. Therefore, the transmission efficiency of all coils that meet the requirements under the misalignment conditions is calculated, and some of the results are selected and shown in Fig. 11. By comparing the different misalignment characteristic curves in Fig. 11, it can be observed that coils A and B correspond to the best and worst transmission characteristics, and the corresponding parameters are N=23, d_x=2.2 mm and N=34, d_x=3.6 mm. The optimal coil parameters obtained through calculation verify the correctness of the optimization results.

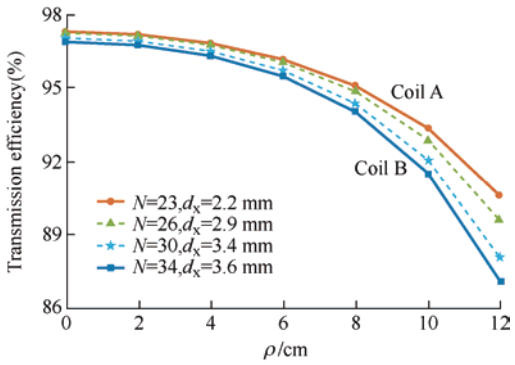

Fig. 11 Calculated value of the coil transmission efficiency variation with the misalignment distance

As illustrated in Tab. 2, compared with the traditional exhaustive attack method, the proposed strategy can save 48.5% of the optimization time, which proves that this method has advantages in improving the efficiency of the coil design. Among them, the optimization time includes the calculation time of the mutual inductance model and the execution time of the algorithm. Additionally, because the FEA method needs to manually rebuild the three-dimensional physical model after the coil parameters are changed, it is time-consuming and has a low efficiency, thus it is not compared with the optimization strategy.

Tab. 2 Comparison of the optimization time

Methods	Exhaustive attack method	Proposed method
Optimization time/h	5.34	2.75

6 Experimental verification

In this section, the transmission characteristics of the designed coils are experimentally verified. Fig. 12 shows the system circuit topology, which includes the DC voltage source, inverter, TX and RX coils, rectifier and compensating capacitor, etc. The experimental prototype of the WPT system is shown in Fig. 13. The DC power supply regulation range is 0-400 V, the inverter is an integrated circuit system based on the GaN semiconductor, and the electronic load is IT8814.

Coil A is the designed coil with the best transmission characteristics to conduct a comparative experiment with coil B. The comparison of the specific coil parameters is presented in Tab. 3. It can be observed that coil A has a greater mutual inductance but a shorter wire length than coil B.

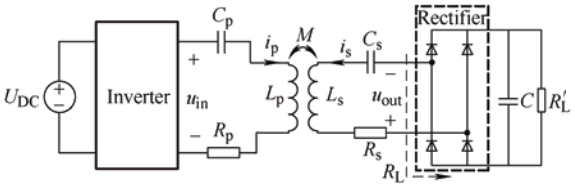

Fig. 12 Circuit structure of WPT system based on SS compensation network

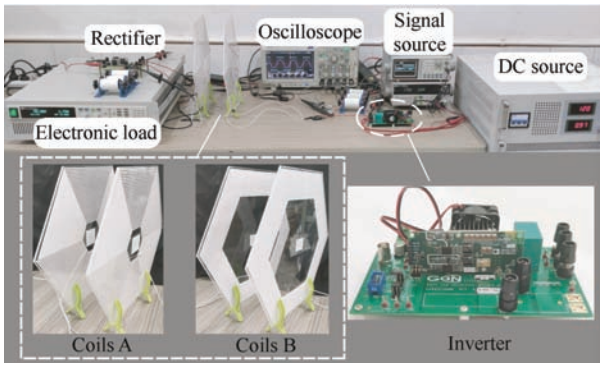

Fig. 13 Experimental platform of the WPT system

Tab. 3 Comparison of specific coil parameters

Parameter	Coil A	Coil B
Side length c_1/cm	18	18
Wire diameter W_a/mm	2	2
Turns N	23	34
Turn spacing d_x/mm	2.2	3.6
Wire length l/m	20.24	22.73
Mutual inductance M/μH	53.5	52.00
Self-induction L_p/L_s/μH	230.2	215.1
Compensation capacitor C_p/C_s/nF	15.2	16.3

6.1 Comparison of transmission characteristics

According to the design requirements of Tab. 1, the transmission distance between the coils should be kept at 10 cm. The relationship between the equivalent resistance of the rectifier input R_L and load R'_L in Fig. 12 is as follows [23]

$$R_L = \frac{8}{\pi^2} R'_L \tag{20}$$

The electronic load and DC power supply are then adjusted so that the equivalent load R_L is 30 Ω and the output power is maintained at 500 W. The voltage and current waveforms of the primary and secondary sides of two sets of the coils are obtained respectively, as shown in Fig. 14. It is deduced that the transmission efficiencies of coils A and B are 95.4% and 95.25%, respectively.

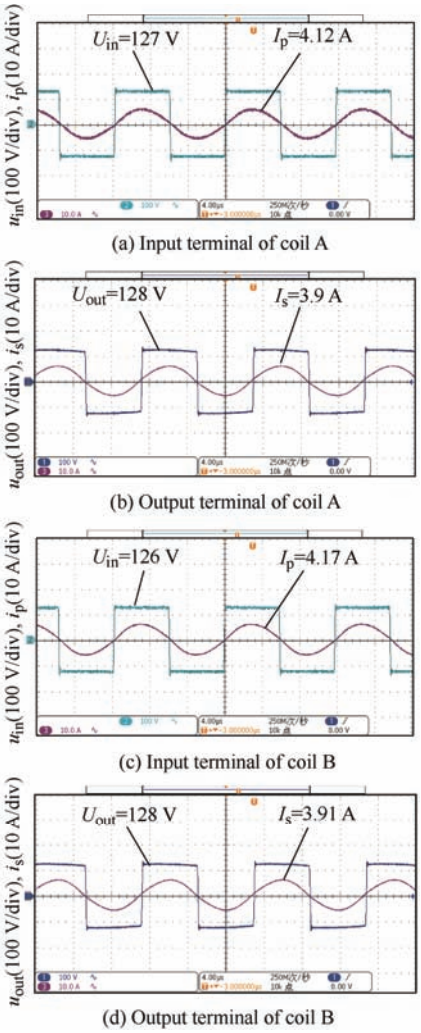

Fig. 14 Experimental comparison of voltage and current waveforms

A comparative experiment is conducted on the misalignment characteristics of coils A and B. The output power is maintained at 500 W when the RX coil is moving, and the experimental results are shown in Fig. 15. It can be observed that the efficiency change trend of the experiment is basically consistent with that shown in Fig. 11. The transmission efficiency of coil A is significantly higher than that of coil B at the same misalignment distance, and the efficiency at the maximum misalignment reaches more than 88%, which reflects excellent transmission characteristics. A small error is observed between the experimental and calculation results in Fig. 11, which is caused by the power loss of the physical modules; however, the maximum error does not exceed 3.06%. The experimental results prove that the mutual inductance model and the proposed optimal design method are reliable.

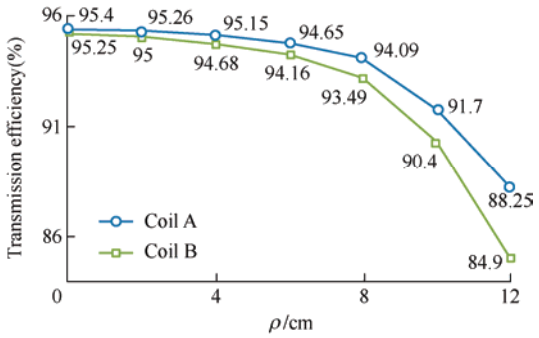

Fig. 15 Experimental results of the transmission efficiency of the misalignment of coils A and B along the tangential boundary

6.2 Misalignment characteristics of the boundary directions

Based on the analysis of Fig. 6, this study considers the misalignment along the tangential boundary as an example to analyze and design the hexagonal coil. Therefore, the misalignment characteristics of the hexagonal coils along the two boundary directions are verified experimentally, and the experimental data are presented in Tab. 4. It can be observed that the transmission efficiency of the coils is very close in the two misalignment directions, which verifies the consistency of the misalignment characteristics of the hexagonal coils along the tangential and central boundaries.

Tab. 4 Experimental results of the coil transmission efficiency in different misalignment directions

Misalignment distance/cm	Efficiency of coil A (%)		Efficiency of coil B (%)	
	ρ	δ	ρ	δ
0	95.4	95.4	95.25	95.25
2	95.26	95.3	95	94.96
4	95.15	95.1	94.68	94.64
6	94.65	94.44	94.16	94.26
8	94.09	93.9	93.49	93.12
10	91.7	91.3	90.4	90.21
12	88.25	88.2	84.93	84.9

7 Conclusions

This study focused on improving the transmission characteristics of the hexagonal coil WPT system and based on the deduced objective function and constraint conditions, a strategy using the GA to automatically realize the multi-parameter optimal design of the coil was proposed. Because the traditional exhaustive attack methods rely too much on the accuracy and dimensions of the parameters, the optimization method proposed in this study obtained the optimal parameters faster and with higher accuracy. The experimental results verified the effectiveness of the proposed optimal design method and improved the transmission characteristics of the WPT system. The proposed coil design method could achieve multi-objective and multi-parameter optimization of the WPT system. On the basis of meeting the actual requirements of the system efficiency and power, the misalignment tolerance of the coils could be improved to a certain extent through the automatic optimization of the number of coil turns and turn spacing, which expanded the optimal design method of the coil parameters. In future work, the influence of the coil parameters on the quality factor and electromagnetic environment will be further considered to form a more reasonable coil optimal design method. Moreover, the method can also be transplanted to applications such as multi-transmitter multi-receiver coils and irregular coils, to solve the optimization design problem of complex coils.

References

[1] B Kallel, O Kanoun, H Trabelsi. Large air gap misalignment tolerable multi-coil inductive power transfer for wireless sensors. *IET Power Electronics*, 2016, 9(8): 1768-1774.

[2] J Sampath, A Alphones, D M Vilathgamuwa. Figure of merit for the optimization of wireless power transfer system against misalignment tolerance. *IEEE Transactions on Power Electronics*, 2017, 32(6): 4359-4369.

[3] Y Yang, J Cui, X Cui. Design and analysis of magnetic coils for optimizing the coupling coefficient in an electric vehicle wireless power transfer system. *Energies*, 2020, 13(16): 4143.

[4] K Song, G Yang, Y Guo, et al. Design of DD coil with high misalignment tolerance and low EMF emissions for wireless electric vehicle charging system. *IEEE Transactions on Power Electronics*, 2020, 35(9): 9034-9045.

[5] T Noda, T Nagashima, H Sekiya. A design of inductively coupled wireless power transfer system with coupling coil optimization. *2015 IEEE International Telecommunications Energy Conference (INTELEC)*, 18-22 October, 2015, Osaka, Japan. IEEE, 2016: 1-6.

[6] Z Zhao, Z Yang, F Lin, et al. Coil optimization of wireless power transfer system applied in trams based on parking wrror law. *Proceedings of the CSEE*, 2017, 37: 196-203.

[7] Y Fang, M Pong. A Bayesian optimization and partial element equivalent circuit approach to coil design in inductive power transfer systems. *2018 IEEE PELS Workshop on Emerging Technologies: Wireless Power Transfer (WoW)*, 03-07 June, 2018, Montreal, QC, Canada. IEEE, 2018: 3-7.

[8] R J Liu, J Wang, J Y Shen. An optimal design of resonant coils for wireless power transfer system based on improved artificial bee colony algorithm. *Applied Mechanics & Materials*, 2014, 614: 168-171.

[9] P Tan, T Peng, X Gao, et al. Flexible combination and switching control for robust wireless power transfer system with hexagonal array coil. *IEEE Transactions on Power Electronics*, 2021, 36(4): 3868-3882.

[10] W Chen, C Liu, C H T Lee, et al. Cost-effectiveness comparison of coupler designs of wireless power transfer for electric vehicle dynamic charging. *Energies*, 2016, 9(11): 906.

[11] I U Castillo-Zamora, P S Huynh, D Vincent, et al. Hexagonal geometry coil for a WPT high-power fast charging application. *IEEE Transactions on Transportation Electrification*, 2019, 5(4): 946-956.

[12] Y Wang, F Lin, Z Yang, et al. Analysis of the influence of compensation capacitance errors of a wireless power transfer system with SS topology. *Energies*, 2017, 10(12): 2177.

[13] P Qi, J Xu, F Yi, et al. The characteristic analysis of magnetically coupled resonant wireless power transmission based on SS compensation structure. *2017 First International Conference on Electronics Instrumentation & Information Systems (EIIS)*, 03-05 June, 2017, Harbin, China. IEEE, 2017: 1-4.

[14] L Yang, J Fan, T Zuo, et al. Simulation study on series model of wireless power transfer via magnetic resonance coupling. *2017 IEEE 3rd Information Technology and Mechatronics Engineering Conference (ITOEC)*, 03-05 October, 2017, Chongqing, China. IEEE, 2017: 191-195.

[15] K Andre, K Aresteidis, M Robert, et al. Wireless power transfer via strongly coupled magnetic resonances. *Science*, 2007, 317(5834): 83-86.

[16] T Mizuno, S Enoki, T Asahina, et al. Reduction of proximity effect in coil using magnetoplated wire. *IEEE Transactions on Magnetics*, 2007, 43(6): 2654-2656.

[17] T Mizuno, S Yachi, A Kamiya, et al. Improvement in efficiency of wireless power transfer of magnetic resonant coupling using magnetoplated wire. *IEEE Transactions on Magnetics*, 2011, 47(10): 4445-4448.

[18] H Tavakkoli, E Abbaspour-Sani, A Khalilzadegan, et al. Analytical study of mutual inductance of hexagonal and octagonal spiral planer coils. *Sensors and Actuators A Physical*, 2016, 247: 53-64.

[19] X Mou, O Groling, H Sun. Energy efficient and adaptive design for wireless power transfer in electric vehicles. *IEEE Transactions on Industrial Electronics*, 2017, 64(9): 7250-7260.

[20] X Wang, Y Wang, Y Liang, et al. Study on the transmission characteristics of magnetic resonance wireless power transfer system. *International Journal of Microwave and Wireless Technologies*, 2017, 9(9): 1-9.

[21] P Tan, Y Fu, C Liu, et al. Modeling of mutual inductance for hexagonal coils with horizontal misalignment in wireless power transfer. *2018 IEEE Energy Conversion Congress and Exposition (ECCE)*, 23-27 September, 2018, Portland, OR, USA. IEEE, 2018: 1981-1986.

[22] J S Jin, S Jung, J K Han. Development of wireless power transmission system for transfer cart with shortened track. *Applied Sciences*, 2020, 10(14): 4694.

[23] O Trachtenberg, A Shoihet, E Beer, et al. Quadrature demodulator based output voltage and load estimation of a resonant inductive WPT link. *2019 IEEE PELS Workshop on Emerging Technologies: Wireless Power Transfer (WoW)*, 18-21 June, 2019, London, UK. IEEE, 2019: 81-84.

Ping'an Tan received the B.S. degree in Automation from Xiangtan University, Xiangtan, China, in 2001, the M.S. degree in Power Electronics from Xiangtan University, Xiangtan, China, in 2004, and the Ph.D. degree in Power Electronics from South China University of Technology, Guangzhou, China, in 2010. He is currently an Associate Professor in the School of Automation and Electronic Information, Xiangtan University, Xiangtan, China. His current research interests include the fields of wireless power transfer, power electronics, and intelligent control.

Bin Song received the B.S. degree in Building Electricity and Intelligence from Xiangtan University, China, in 2019, where he is currently working toward the M.S. degree in Power Electronics. His research interests include wireless power transfer applications and power electronics converters.

Xu Shangguan received his B.S. degree in Electric Engineering and Automation from the Hunan Institute of Engineering, Xiangtan, China, in 2019. He is presently working towards his M.S. degree in Electrical Engineering at Xiangtan University, Xiangtan, China. His current research interests include wireless power transmission applications and electromagnetic compatibility.

Huadong Liu received his B.S. degree in Electrical Engineering and Automation from the Chengdu University of Technology, Chengdu, China, in 2005; and his M.S. degree from Southwest Jiaotong University, Chengdu, China, in 2008. In 2008, he joined the CRRC Zhuzhou Institute Co., Ltd., Zhuzhou, China. He is presently working as a Senior Engineer at the CRRC ZIC Research Institute of Electrical Technology and Material Engineering. His current research interests include wireless power transfer system design, converter control design, and programming techniques and languages.